Application of Object-Based Image Analysis for Detecting and Differentiating between Shallow Landslides and Debris Flows

Helen Cristina Dias[1], Daniel Hölbling[2], Vivian Cristina Dias[1], Carlos Henrique Grohmann[1]

[1]University of São Paulo (IEE-USP), São Paulo, Brazil
[2]University of Salzburg, Salzburg, Austria

Abstract

Mass movement mapping is essential for susceptibility, vulnerability and risk assessments. Various mapping approaches based on Earth observation (EO) data have been used to identify different types of hazards. Object-based image analysis (OBIA) has been employed for EO-based landslide mapping worldwide. The development and application of efficient methods for recognition and mapping are essential to create standards for landslide inventory mapping, notably in Brazil where landslides are a frequent natural hazard. This study aims to detect landslide features and differentiate them into shallow landslides and debris flows using a semi-automated OBIA approach. RapidEye satellite images (5 m) were analysed and the Normalized Difference Vegetation Index (NDVI) was calculated. A Digital Elevation Model (DEM) (12.5 m) and its derived products were integrated into the analysis to support the OBIA landslide mapping. The results show that the method is suitable for the recognition of this type of hazard and are potentially of use for local stakeholders and decision-makers in disaster management.

Keywords:

mass movement, landslide inventory, object-based image analysis, semi-automated mapping

1   Introduction

Landslides are a major natural hazard worldwide. They occur under varied climatic conditions and in different types of landscape, cost billions of dollars to manage and repair and in terms of financial losses, and are responsible for thousands of deaths and injuries every year (Highland and Bobrowsky, 2008). Creating a landslide inventory is the first and main step for susceptibility, vulnerability and risk analysis, and it should be noted that the accuracy of any inventory has a direct effect on the efficiency of subsequent studies. Manual, semi-automated and automated methods have been used to identify and map this type of hazard (Carou et al., 2017; Hölbling et al., 2017; Barella et al., 2019; Comert et al., 2019; Canavesi et al., 2020; Karantanellis et al., 2021; Dias et al., 2021c; Soares et al., 2022; Liang et al., 2022). Object-

based image analysis (OBIA) has a high potential for landslide recognition in satellite imagery (Martha et al., 2010; Hölbling et al., 2017; Comert et al., 2019; Hölbling, 2022). It allows spatial and spectral information (e.g. shape, texture, contextual and morphological information) to be used for object segmentation and classification (Blaschke, 2010). It has been demonstrated that the method is suitable for landslide detection and classification in different environments using different remote sensing data (Hölbling, 2022). The method also enables the differentiation between shallow landslides and debris flows (Hölbling et al., 2015). However, semi-automated differentiation between different mass movement types is not common and only a few OBIA studies have proposed such approaches (Hölbling et al., 2012, 2015; Eisank et al., 2014a; Plank et al., 2015; Heleno et al., 2016).

In Brazil specifically, semi-automated and automated mapping of shallow landslides and debris flows is not often performed, although 37% of rainfall-triggered landslides in South America occur there (Froude & Petley, 2018). Despite the high landslide frequency, Brazilian landslide inventories are poorly developed (Dias et al., 2021a, 2021b), and recognition and mapping are mainly done manually through image interpretation (Dias et al., 2021a). This study therefore focuses on an area in Brazil to detect mass movement features, classifying them into shallow landslides and debris flows using OBIA.

2   Materials and Methods

2.1 Study area

The study area is part of the Ribeira Valley region, in the southwestern part of the Serra do Mar in the state of São Paulo (Figure 1). The Guarda-mão basin is located in the municipality of Itaóca and has an area of 7.3 km². It was selected because of the occurrence of numerous shallow landslides and debris flows triggered by an extreme rainfall event on 12–13 January 2014, which caused damage to local infrastructure and economic losses, and lead to 25 deaths and 332 people becoming homeless (Brollo et al., 2015; Gramani and Martins, 2016; Dias et al., 2022). The debris flows themselves were caused by shallow landslides, which provided the initial material (Dias et al., 2022) (Figure 2).

2.2 Data

We used a RapidEye Analytic Ortho Tile multispectral satellite image (5m resolution) dated 30 January 2014. A 1:10,000 scale map of the drainage network from the Geographic and Cartographic Institute of the State of São Paulo (IGC-SP) was used in addition. Supplementary data for slope, curvature and flow accumulation were derived from the pre-event ALOS Digital Elevation Model (DEM) with 12.5m resolution, acquired from the Alaska Satellite Facility. The Normalized Difference Vegetation Index (NDVI) was calculated, an index that has been applied to detect varying densities of vegetation coverage and which is commonly used in landslide studies (Bhandari et al., 2012; Uehara et al., 2020; Soares et al., 2022).
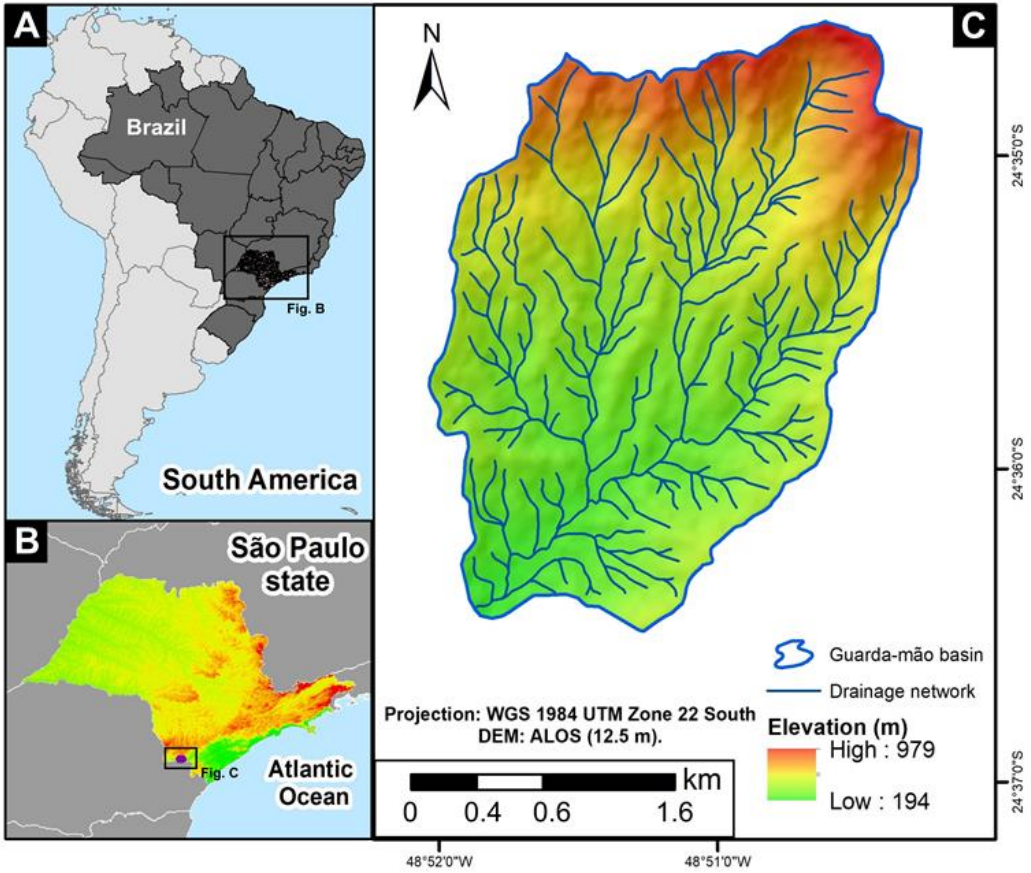
Figure 1: Location of the study area. **A:** Brazil, South America; **B:** São Paulo state; **C:** Guarda-mão basin.

Figure 2: Mass movement event in Itaóca, 2014. **A:** Debris flow and shallow landslides on a steep slope; **B:** Deposition area of mostly coarse material in a valley of the Guarda-mão basin. Source: M.F. Gramani.

2.3 Object-based mass movement mapping

Two types of mass movement occurred in the study area: shallow landslides and debris flows. For semi-automated mapping and differentiation of landslide types, an object-based approach was applied using eCognition 10.0 (Trimble) software. For segmentation, a multiresolution segmentation algorithm was used. The algorithm identifies singular objects and merges them with their neighbours, based on a homogeneity criterion, which is a combination of spectral and shape parameters (Benz et al., 2004). The segmentation settings were as follows: scale parameter: 50; shape: 0.3; compactness: 0.9. They were defined based on expert knowledge and trial and error, with the aim of creating image objects that suited landslide recognition in our study site.

The recognition, differentiation and classification (Table 1) of shallow landslides and debris flows were based mainly on three different metrics: spatial ('distance' and 'border to'), spectral (NDVI), and morphological (slope and flow accumulation). Classification thresholds were determined and adjusted based on expert knowledge. According to the literature (Varnes, 1978; Cruden & Varnes, 1996; Highland & Bobrowsky, 2008; Hungr et al., 2014), shallow landslides are common on steep slopes and can trigger debris flows near and in stream channels. These characteristics were essential for the construction of the classification rule set in eCognition.

Table 1: Classification parameters and thresholds used in OBIA.

Mass movement type	Classification parameters
Shallow landslide	Mean NDVI ≤ 0.32 Mean slope ≥ 16 Distance to drainage network ≥ 12 m Border to drainage network ≥ 0.5 m
Debris flow	Mean NDVI ≤ 0.32 Mean slope ≤ 16 Distance to drainage network ≤ 1 m Border to drainage network ≤ 0.5 m

Based on the mapping results, morphological information of the mass movement type characteristics was derived from the ALOS DEM. The slope and plan curvature were analysed, and the respective means were calculated.

2.4 Accuracy assessment

The accuracy of the results was assessed by comparison with a shallow landslide and debris flow inventory, created through expert interpretation (Dias et al., 2022) by considering the spatial overlap between the reference and the semi-automated OBIA classification. The samples (501) were split equally into three categories (167 samples each): shallow landslides, debris flows and non-landslides. The accuracy was assessed by determining the numbers of

true positives (TP), false positives (FP), true negatives (TN), and false negatives (FN), and translated into Producer's accuracy (PA), User's accuracy (UA), Overall Accuracy (OA), and F1 Score. TP represents objects correctly classified; FP represents objects wrongly classified; TN represents objects correctly not classified as shallow landslide or debris flow; FN represents objects incorrectly not classified as shallow landslide or debris flow. PA indicates the probability that a given object has been correctly classified, and UA indicates the probability that a classified object actually represents this class (Dias et al., 2021c). In addition, spatial accuracy metrics were applied (Eisank et al. 2014b; Hölbling et al., 2017).

The OBIA classification was based on the initial segmentation. These objects were suitable for the classification of areas affected by landslides, but due to the variability of landslides it is difficult to delineate landslides as single objects and thus to identify the number of landslides (Hölbling et al., 2016). Due to over-segmentation, the delineation of the objects did not agree with the manual landslide delineation (e.g. one manually identified landslide might contain several smaller OBIA objects). Therefore, objects classified as landslides using OBIA were merged into larger polygons based on proximity and contiguity. This allowed a geometric comparison of the object delineations, and five spatial accuracy metrics were calculated: (1) Quality Rate (QR), (2) Area Fit Index (AFI), (3) Over-Segmentation Rate (OR), (4) Under-Segmentation Rate (UR), and (5) Root mean square (D). These metrics rely on the area proportions, with a range of values between 0 and 1 (except for AFI). The closer the value is to zero, the better the spatial match between the test and reference datasets (Eisank et al. 2014b; Hölbling et al., 2017). Equations for the spatial accuracy metrics can be found in Eisank et al. (2014b).

3 Results and discussion

3.1 Differentiating between shallow landslides and debris flows using OBIA

Figure 3 shows the results of the semi-automated object-based classification of shallow landslides and debris flows. Generally, the semi-automated classification generates lower totals than the reference mapping. A total area of 215,125 m² (128 polygons after merging) was classified as shallow landslides, whereas the reference mapping showed 292,980 m² (149 polygons). For debris flows, an area of 234,275m² (13 polygons after merging) was classified by OBIA, and 295,427 m² (2 polygons) were mapped in the reference.

The differences between the semi-automatically classified shallow landslides and debris flows and the reference amount to approximately 27% and 21% of the areas respectively. The classification of debris flows showed slightly better accuracy than that of shallow landslides (Table 2). This may result from the differences in the morphological characteristics of landslides and debris flows. Debris flows create a clear path of erosion due to entrainment, which mobilizes most of the sediments and materials present in the streams (e.g., boulders and logs). The larger size of debris flows in comparison to small shallow landslide scars favours their identification through both methods (manual and semi-automatic). The major debris flow initiated in the Guarda-mão reached the Palmital river and caused damage to downtown Itaóca (Dias et al., 2022).

The accuracy metrics produced results similar to those reported in the literature (Hölbling et al., 2015; Dias et al., 2021c; Soares et al., 2022), namely for shallow landslides an F1 Score of 78% and an OA of 87; and for debris flows an F1 score of 86% and an OA of 89%. Satisfactory results were achieved for the spatial accuracy metrics. By merging the OBIA classification objects, it was possible to compare the total number of semi-automatically classified landslides with the manual mapping. However, some small shallow landslides were missed by OBIA, some neighbouring landslides were incorrectly merged into a larger polygon, and fragmentation of specific debris flow sectors occurred. Nevertheless, the geometric comparison of the final landslide objects indicated a good to high agreement between the reference inventory and the OBIA mapping, with most of the spatial indices showing values below 0.5 (Table 2). For debris flows, a better spatial agreement was obtained between the reference and OBIA polygons than for landslides, which was confirmed by the other accuracy metrics (PA, UA, F1 Score and OA). Although the OBIA debris flows were more fragmented (i.e. there were more polygons), the delineations of large sectors in the centre-north of the Guarda-mão basin matched well.
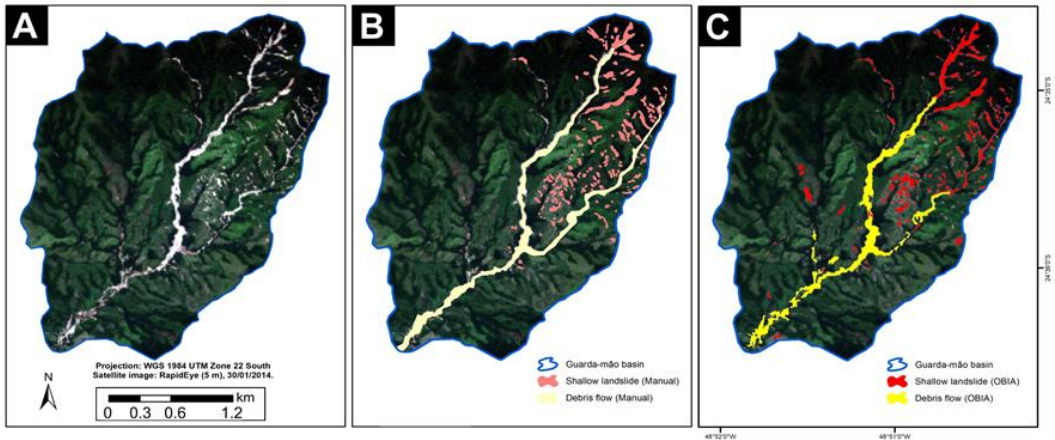
Figure 3: Comparison of manual and OBIA mapping in the Guarda-mão basin. **A:** RapidEye image of the Guarda-mão basin after the mass movement event in 2014; **B:** Manual mapping of shallow landslides and debris flows; **C:** Identification of shallow landslides and debris flows using OBIA.

Table 2: Accuracy assessment results.

	Shallow landslide	Debris flow
PA (%)	66	95
UA (%)	95	79
F1Score (%)	78	87
OA (%)	87	89
QR	0.66	0.51
AFI	0.26	0.21
OR	0.56	0.41
UR	0.40	0.25
D	0.48	0.33

3.2 Mass movement type characteristics

Morphological and spectral analyses were performed to reveal the different characteristics of the shallow landslides and debris flows. Three parameters were analysed: slope, curvature and NDVI. Table 3 shows the mean values of each parameter. Slope presented very distinct means: 24° and 6.8°, for shallow landslides and debris flows respectively. Shallow landslides are prone to occur on slopes ≥ 20° (Fernandes et al., 2001; Zhou et al., 2002), while debris flows are directly related to stream channels (Costa, 1984; VanDine, 1996; Jakob, 2005). Both processes present a negative value for curvature; a negative result indicates that the pre-event surface was concave and responsible for converging materials and flows (Fernandes et al., 2001; Dias et al., 2017; Martins et al., 2017). NDVI means were similar for both processes. The NDVI was very useful for identifying mass movements in the first step, because both processes lead to the exposure of bare ground with no or sparse vegetation (NDVI ≤−0.2). However, differentiation between shallow landslides and debris flows based on the NDVI was not possible.

Table 3: Morphological and spectral characteristics of shallow landslides and debris flows in the Guarda-mão basin.

Characteristics	Parameters	Shallow landslides (means)	Debris flows (means)
Morphology	Slope	24°	6.8°
	Curvature	-0.31	-0.34
Spectral	NDVI	0.18	0.11

3.3 Common classification errors

The object-based method proved to be suitable for the identification and differentiation of shallow landslides and debris flows. Nonetheless, some errors occurred, mostly false positives – in other words, objects that were wrongly classified (Figure 4). The main FP errors were related to non-vegetated areas other than mass movements (Figures 4A and B), stream channels (Figure 4B), and debris flows incorrectly classified as shallow landslides (Figure 4C). The false negative objects were mainly small shallow landslide features (Figure 4D) and specific debris flow sectors (Figure 4E). These findings are similar to those of other remote sensing-based landslide mapping studies in Brazil. These studies include Dias et al. (2021c), who applied three pixel-based algorithms in São Paulo state and found that the most common errors were related to non-vegetated areas, such as pasture classified as landslides, or clouds and stream channels. The same authors also reported difficulties in classifying small landslide scars. Soares et al. (2022) applied a deep learning method in the states of Rio de Janeiro and Rio Grande do Sul and mentioned challenges in landslide detection: their model confuses streams, bare soil, roads and roofs. In general, shallow landslides and debris flows have almost the same spectral responses and NDVI values. This explains the misunderstanding regarding the case shown in Figure 4C. Steep slopes are prone to shallow landslides and, in some cases, show the same conditions as where debris flows initiate. As most debris flows are triggered by

shallow landslides, it is important to evaluate where one process ends and another begins. The comparison between pre- and post-event images of the affected area allows the expert to identify the initiation zone (in this case, the landslide which triggered the process). Unfortunately, in our study, the rule set could not always differentiate between the two processes if they occurred under similar morphological conditions. The investigator's expertise is therefore crucial in correctly identifying the features.
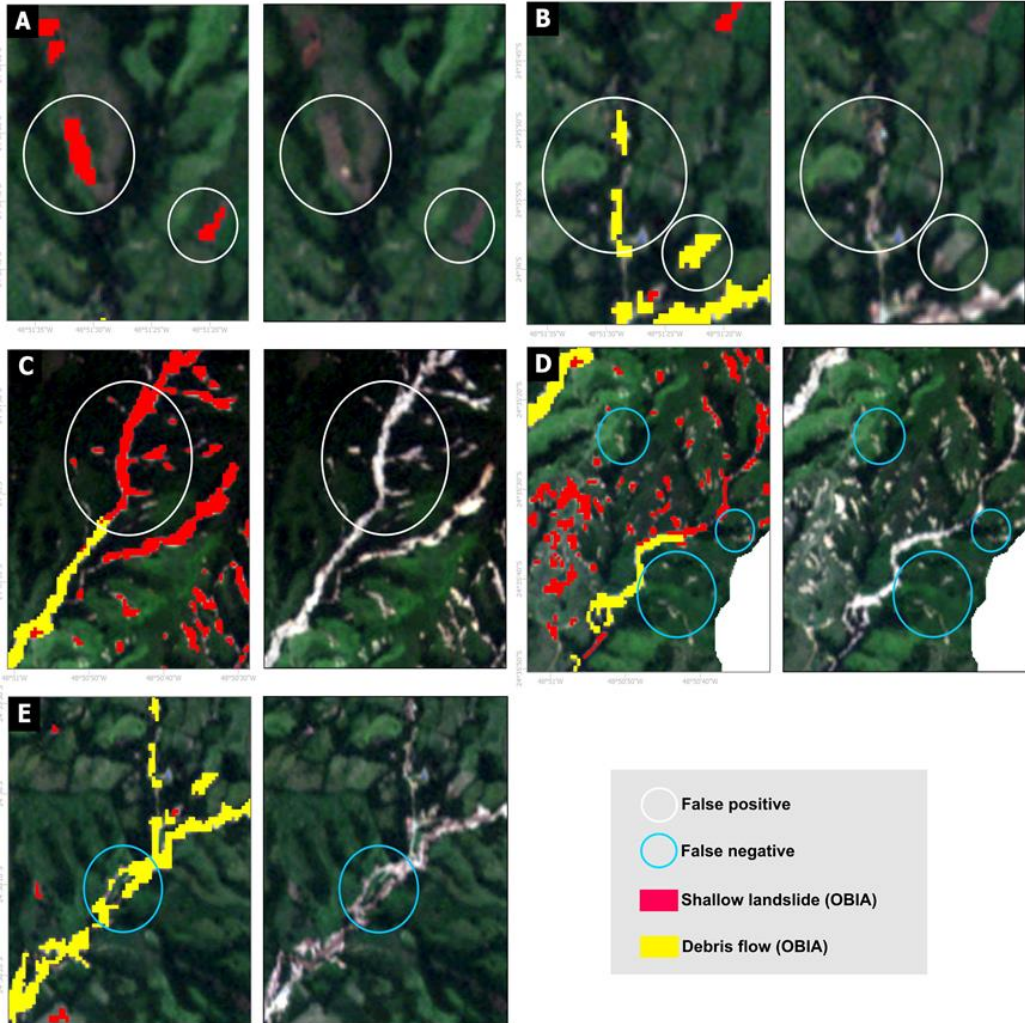
Figure 4: Classification errors (false positives and false negatives). **A:** Non-vegetated areas wrongly classified as shallow landslides; **B:** Stream channels wrongly classified as debris flows; **C:** Debris flow wrongly classified as shallow landslides; **D:** Small shallow landslides not classified by OBIA; **E:** Debris flow not classified by OBIA.

4   Conclusion

An object-based approach for shallow landslide and debris flow classification was applied in Itaóca, southeastern Brazil. Spatial, spectral and morphological information was used for the segmentation and classification of objects using a high-resolution satellite image. The results showed that the method is suitable for identifying this type of hazard. The classification correctly identified more than 70% of all shallow landslides and debris flows. The errors were concentrated in non-vegetated areas and stream channels, and were due to confusion between the two classes. In addition, very small shallow landslides were not identified by the method. In future studies, improvements could be achieved by using higher resolution EO data, which would give greater mapping accuracy and avoid common classification errors. Multi-temporal analysis based on NDVI changes could also improve mapping accuracy. The results could be useful for local stakeholders and decision-makers, as information on the location and spatial distribution of landslides is important in disaster management. As the first application of OBIA in the Serra do Mar Paulista, a mountain range heavily affected by mass movements, this study contributes to improving approaches to mass movement mapping in Brazil and elsewhere.

Acknowledgements

References

Barella, C. F., Sobreira, F. G., and Zêzere, J. L. (2019). A comparative analysis of statistical landslide susceptibility mapping in the southeast region of Minas Gerais state, Brazil. Bulletin of Engineering Geology Environment, 78, 3205–3221.

Benz, U. C., Hofmann, P., Willhauck, G., Lingenfelder, I., and Heynen, M. (2004). Multi-resolution, object-oriented fuzzy analysis of remote sensing data for GIS-Ready information. PRS Journal of Photogrammetry and Remote Sensing, 58, 239–258.

Bhandari, A. K., Kumar, A., and Singh, G. K. (2012). Feature extraction using normalized difference vegetation index (NDVI): A study of Jabalpur city. Procedia Technology, 6, 612–621.

Blaschke, T. (2010). Object-based image analysis for remote sensing. ISPRS journal of photogrammetry and remote sensing, 65(1), 2–16.

Brollo, M. J., Santoro, J., Penteado, D. R., da Silva, P. C. F., and Ribeiro, R. R. (2015). Itaóca (sp): Histórico de acidentes e desastres relacionados a perigos geológicos. In XIV Simpósio de Geologia do Sudeste. Campos do Jordão - SP.

Canavesi, V., Segoni, S., Rosi, A., Ting, X., Nery, T., Catani, F., and Casagli, N. (2020). Different approaches to use morphometric attributes in landslide susceptibility mapping based on meso-scale spatial units: A case study in Rio de Janeiro (Brazil). Remote Sensing, 12, 1826.

Carou, C. B., Vieira, B. C., Martins, T. D., and Gramani, M. F. (2017). Inventário dos escorregamentos da bacia do Rio Gurutuba, Vale do Ribeira (SP). Revista do Departamento de Geografia, Especial XVII SBGFA / I CNGF (2017), 172–179.

Comert, R., Avdan, U., Gorum, T., and Nefeslioglu, H. A. (2019). Mapping of shallow landslides with object-based image analysis from unmanned aerial vehicle data. Engineering Geology, 260, 105264.

Costa, J. E. (1984). Developments and applications of geomorphology, chapter Physical Geomorphology of Debris Flows, 268–317. Springer-Verlag.

Cruden, D. M.; Varnes, D. J. (1996): Landslide types and processes. In: Turner, A. K.; Schuster, R. L. (Eds.): Landslides: Investigation and Mitigation. Transportation Research Board Special Report 247. National Research Council, 36-75.

Dias, H. C., Dias, V. C., and Vieira, B. C. (2017). Condicionantes morfológicos e geológicos dos escorregamentos rasos na bacia do Rio Santo Antônio, Caraguatatuba/SP. Revista do Departamento de Geografia, page 157.

Dias, H. C., Hölbling, D., and Grohmann, C. H. (2021a). Landslide inventory mapping in Brazil: Status and challenges. In XIII Internacional Symposium on Landslides. Cartagena, Colombia.

Dias, H. C., Hölbling, D., and Grohmann, C. H. (2021b). Landslide susceptibility mapping in Brazil: A review. Geosciences, 11:425.

Dias, H. C., Sandre, L. H., Alarcón, D. A. S., Grohmann, C. H., and Quintanilha, J. A. (2021c). Landslide recognition using SVM, random forest, and maximum likelihood classifiers on high-resolution satellite images: A case study of Itaóca, southeastern Brazil. Brazilian Journal of Geology, 51.

Dias, V. C., McDougall, S., and Vieira, B. C. (2022). Geomorphic analyses of two recent debris flows in Brazil. Journal of South American Earth Sciences, 113:103675.

Eisank, C., Hölbling, D., Friedl, B., Chen, Y.-C., and Chang, K.-T. (2014a). Expert knowledge for object-based landslide mapping in Taiwan. South-Eastern European Journal of Earth Observation and Geomatics, Special Thematic Issue: GEOBIA 2014 - Advancements, trends and challenges, 3(2S), 347–350.

Eisank, C., Smith, M., and Hillier, J. (2014b). Assessment of multiresolution segmentation for delimiting drumlins in digital elevation models. Geomorphology, 214, 452–464.

Fernandes, N. F., Guimarães, R. F., Gomes, R. A. T., Vieira, B. C., Montgomery, D. R., and Greenberg, H. (2001). Condicionantes geomorfológicos dos deslizamentos nas encostas: Avaliação de metodologias e aplicação de modelo de previsão de áreas susceptíveis. Revista Brasileira de Geomorfologia, 2.

Froude, M. J. and Petley, D. N. (2018). Global fatal landslide occurrence from 2004 to 2016. Natural Hazards and Earth System Science, 18, 2161–2181.

Gramani, M. and Martins, V. (2016). Debris flows occurrence by intense rains at Itaóca city, São Paulo, Brazil: Field observations. In Landslides and Engineered Slopes. Experience, Theory and Practice, 1011–1019. CRC Press.

Heleno, S., Matias, M., Pina, P., and Sousa, A. J. (2016). Semiautomated object-based classification of rain-induced landslides with VHR multispectral images on Madeira Island. Natural Hazards and Earth System Sciences, 16(4), 1035–1048.

Highland, L. and Bobrowsky, P. (2008). The landslide handbook: A guide to understanding landslides (USGS circular 1325). Reston, VA: US Geological Survey.

Hölbling, D. (2022). Data and knowledge integration for object-based landslide mapping – challenges, opportunities and applications. gis.Science - Die Zeitschrift für Geoinformatik, 1:1–13.

Hölbling, D., Betts, H., Spiekermann, R., Phillips, C., 2016. Identifying Spatio-Temporal Landslide Hotspots on North Island, New Zealand, by Analyzing Historical and Recent Aerial Photography. Geosciences, 6, 48. http://dx.doi.org/10.3390/geosciences6040048

Hölbling, D., Eisank, C., Albrecht, F., Vecchiotti, F., Friedl, B., Weinke, E., and Kociu, A. (2017). Comparing manual and semi-automated landslide mapping based on optical satellite images from different sensors. Geosciences, 7:37.

Hölbling, D., Friedl, B., and Eisank, C. (2015). An object-based approach for semi-automated landslide change detection and attribution of changes to landslide classes in northern Taiwan. Earth Science Informatics, 8(2):327–335.

Hölbling, D., Füreder, P., Antolini, F., Cigna, F., Casagli, N., and Lang, S. (2012). A semi-automated object-based approach for landslide detection validated by persistent scatterer interferometry measures and landslide inventories. Remote Sensing, 4:1310– 1336.

Hungr, O., Leroueil, S., and Picarelli, L. (2014). The Varnes classification of landslide types, an update. Landslides, 11, 167-194.

Jakob, M. (2005). Debris-flow hazards and related phenomena, chapter Debris-flow hazard analysis, 411–443. Springer, Berlin.

Karantanellis, E., Marinos, V., Vassilakis, E., and Hölbling, D. (2021). Evaluation of machine learning algorithms for object-based mapping of landslide zones using UAV data. Geosciences, 11, 305.

Liang, X., Segoni, S., Yin, K., Du, J., Chai, B., Tofani, V., and Casagli, N. (2022). Characteristics of landslides and debris flows triggered by extreme rainfall in Daoshi town during the 2019 typhoon Lekima, Zhejiang province, China. Landslides, 19, 1735– 1749.

Martha, T. R., Kerle, N., Jetten, V., van Westen, C. J., and Kumar, K. V. (2010). Characterising spectral, spatial and morphometric properties of landslides for semiautomatic detection using object-oriented methods. Geomorphology, 116, 24–36.

Martins, T. D., Oka-Fiori, C., Vieira, B. C., de Barros Correa, A. C., and Bateira, C. V. M. (2017). Análise dos parâmetros morfológicos de escorregamentos rasos na serra do mar, paraná. Caminhos da Geografia, 18, 223–239.

Plank, S., Hölbling, D., Eisank, C., Friedl, B., Martinis, S., and Twele, A. (2015). Comparing object-based landslide detection methods based on polarimetric SAR and optical satellite imagery - a case study in Taiwan. In 7th International Workshop on Science and Applications of SAR Polarimetry and Polarimetric Interferometry POLinSAR 2015, Frascati, Italy, 26-30 January, 5, Frascati, Italy.

Soares, L. P., Dias, H. C., Garcia, G. P. B., and Grohmann, C. H. (2022). Landslide segmentation with deep learning: Evaluating model generalization in rainfall-induced landslides in Brazil. Remote Sensing, 14(9), 2237.

Uehara, T. D. T., Corrêa, S. P. L. P., Quevedo, R. P., Körting, T. S., Dutra, L. V., and Rennó, C. D. (2020). Landslide scars detection using remote sensing and pattern recognition techniques: Comparison among artificial neural networks, gaussian maximum likelihood, random forest, and support vector machine classifiers. Revista Brasileira de Cartografia, 72, 665–680.

VanDine, D. (1996). Debris flow control structures for forest engineering. Technical report, Director of Research, B.C. Ministry of Forests, Victoria, BC.

Varnes, D. J. (1978). Slope movement types and processes. Special report, 176, 11–33.

Zhou, C., Lee, C., Li, J., and Xu, Z. (2002). On the spatial relationship between landslides and causative factors on Lantau Island, Hong Kong. Geomorphology, 43(3-4), 197–207.